Supporting Information

Rawson et al. 10.1073/pnas.1708839115

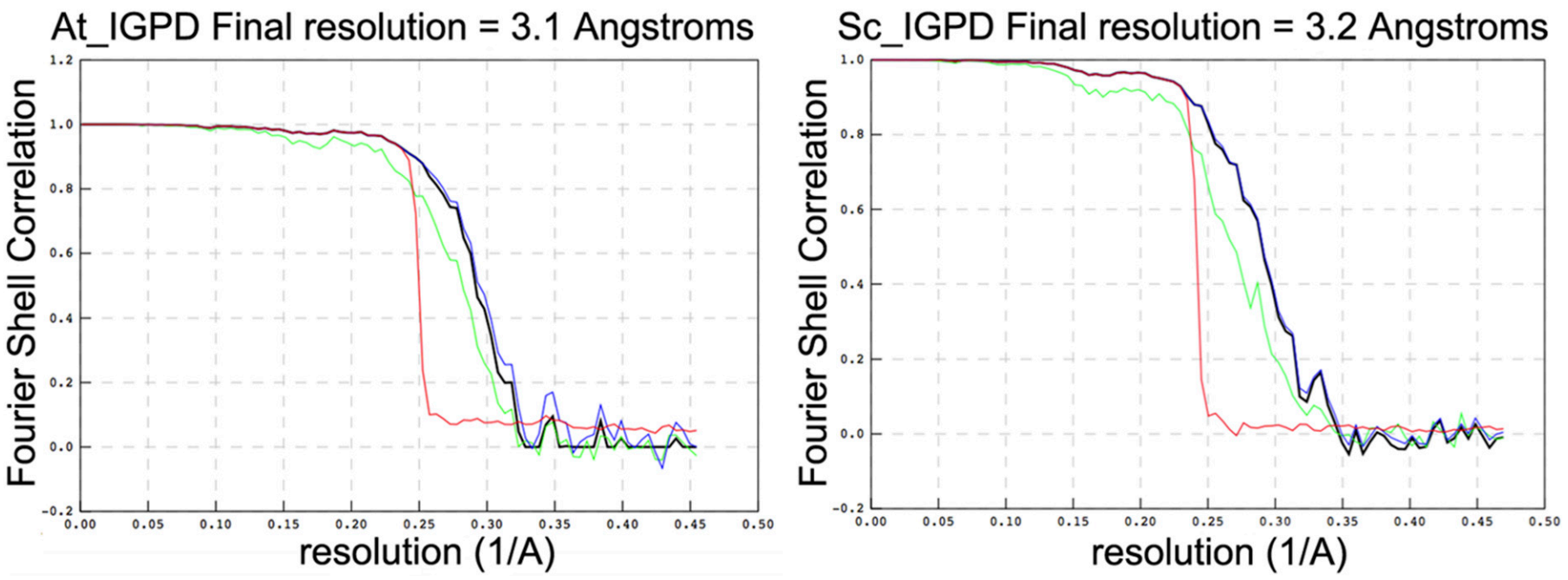

Fig. S1. Fourier shell correlation (FSC) curves for the *At*_IGPD and *Sc*_IGPD maps. Gold standard FSC curves for the *At*_IGPD (*Left*) and *Sc*_IGPD (*Right*) reconstruction at 3.1- and 3.2-Å resolution, respectively. The curves show the Fourier shell correlation for the corrected maps (black), unmasked maps (green), masked maps (blue), and phase randomized maps (red).

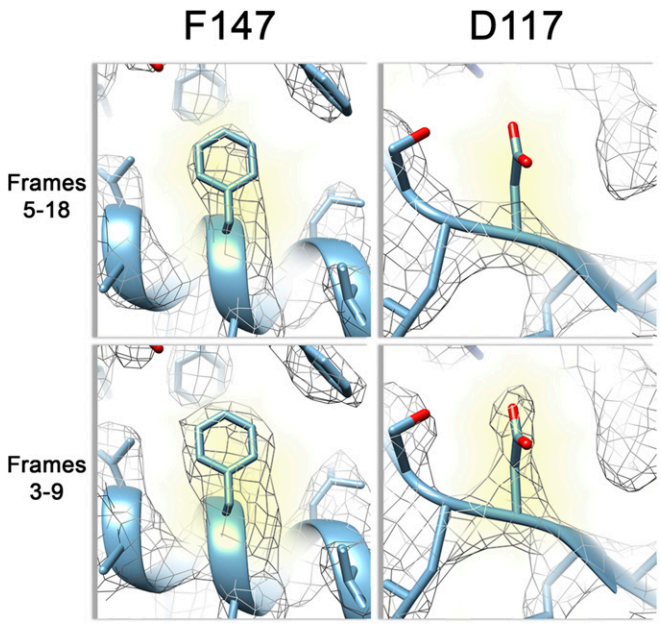

Fig. S2. Analysis of the effect of radiation damage on the *At*_IGPD EM map. Difference in the strength of the density around Asp117 when the exposure dose is reduced to minimize radiation damage. A higher dose for frames 5–18 results in an absence of density; however, cutting back the dose to just frames 3–9 restores the density. In both cases, F147 (*Left*) is taken as a reference and contoured to the same level as Asp117 (*Right*).

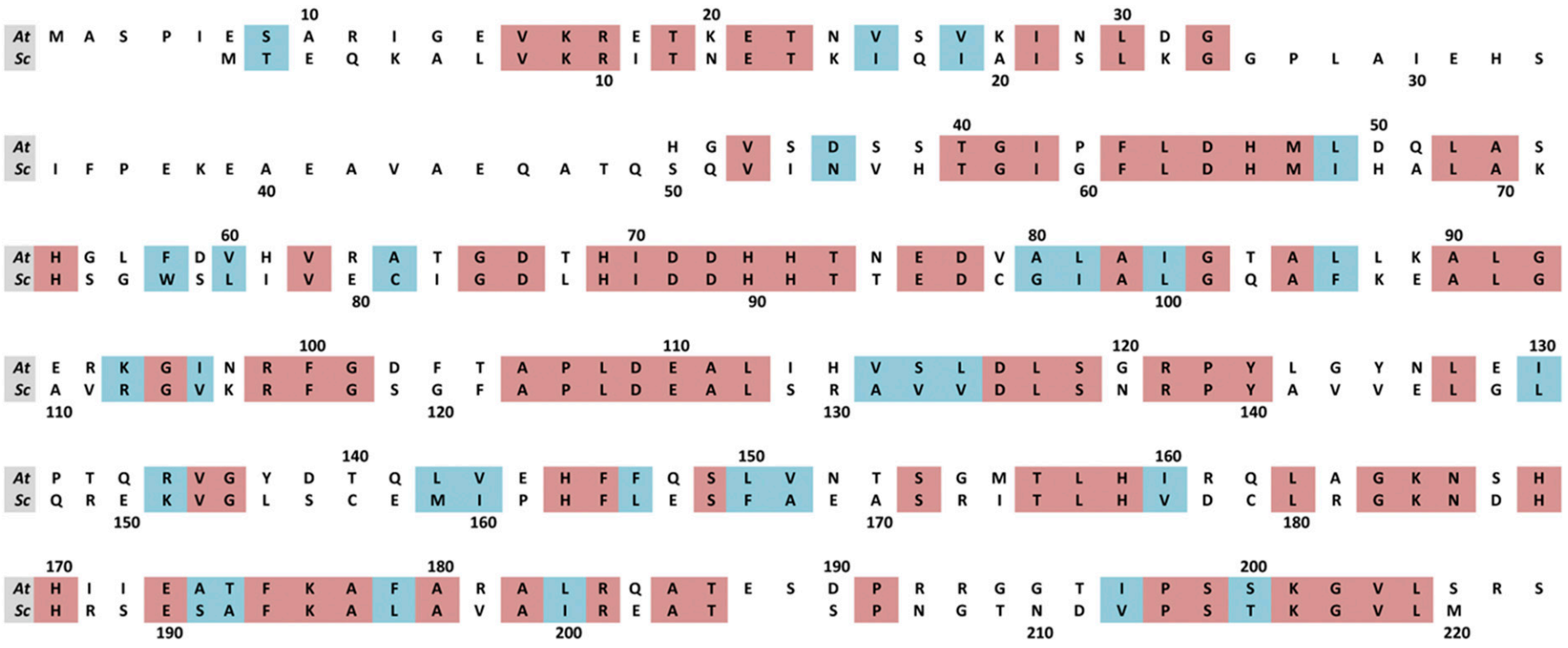

Fig. S3. Sequence alignment of both *At* and *Sc*_IGPD. An alignment for IGPD from both *A. thaliana* (At) and *S. cerevisiae* (Sc) with numbering above and below the alignment, respectively. Those residues fully conserved are boxed in red, and those that are similar are boxed in blue.

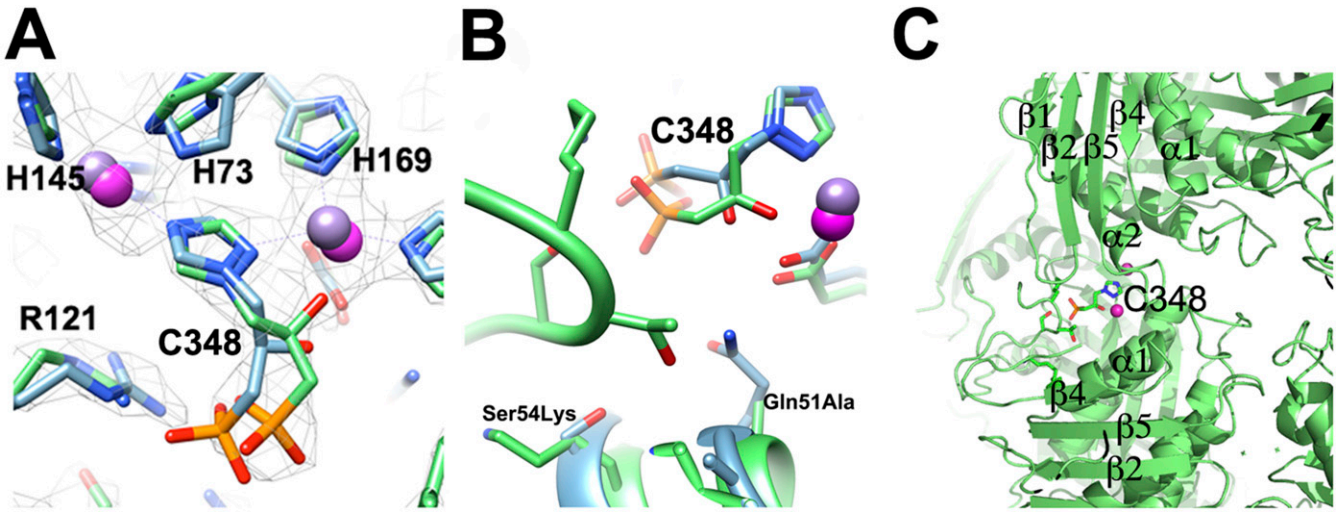

Fig. S4. Analysis of the difference within the *At* and *Sc*_IGPD inhibitor binding sites. (*A*) Comparison of the *At*_IGPD (blue) and *Sc*_IGPD (green) active site, with key residues and inhibitor shown in stick format. Mn^{2+} ions are shown as purple (*At*_IGPD) or magenta (*Sc*_IGPD) spheres; nitrogen, oxygen, and phosphorous are colored blue, red, and orange, respectively. The corresponding map for the *Sc*_IGPD structure is shown showing the quality of fit for the bound inhibitor. (*B*) Alternative view of the inhibitor binding site with those residues that differ between *At*_IGPD and *Sc*_IGPD, shown in stick format (Ser54Lys and Gln51Ala). The color scheme is the same as in *A*, and the numbering relates to *At*_IGPD. (*C*) Overview of the inhibitor binding site in *Sc*_IGPD in the same orientation as *B* to show the position of the binding site with respect to the interface between two monomers. The inhibitor and key residues are shown in stick format.

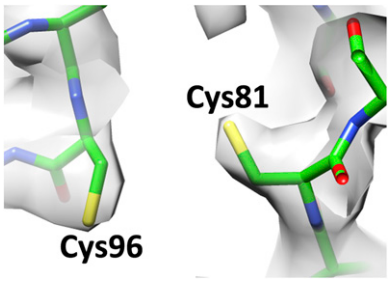

Fig. S5. Analysis of the position of Cys81 and Cys96 in the *Sc*_IGPD EM-derived map. Both Cys81 and Cys96 are located within close proximity; however, they do not form a disulphide bond.

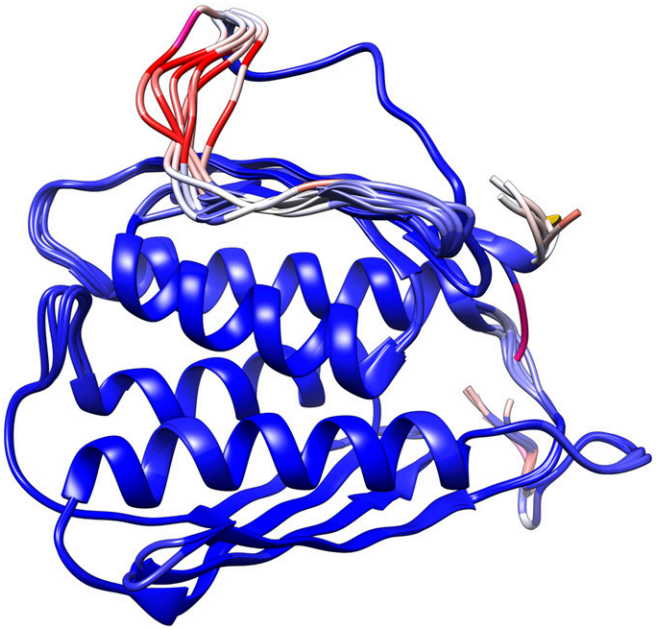

Fig. S6. Loop modeling in *Sc*_IGPD. Analysis of an ensemble consisting of six of the highest scoring models generated, using Rosetta comparative modeling colored by rmsd from blue to red. Ambiguity in the models is concentrated around the termini and between Ser39 to Val43 in the insertion loop where the EM-derived map density is weakest.

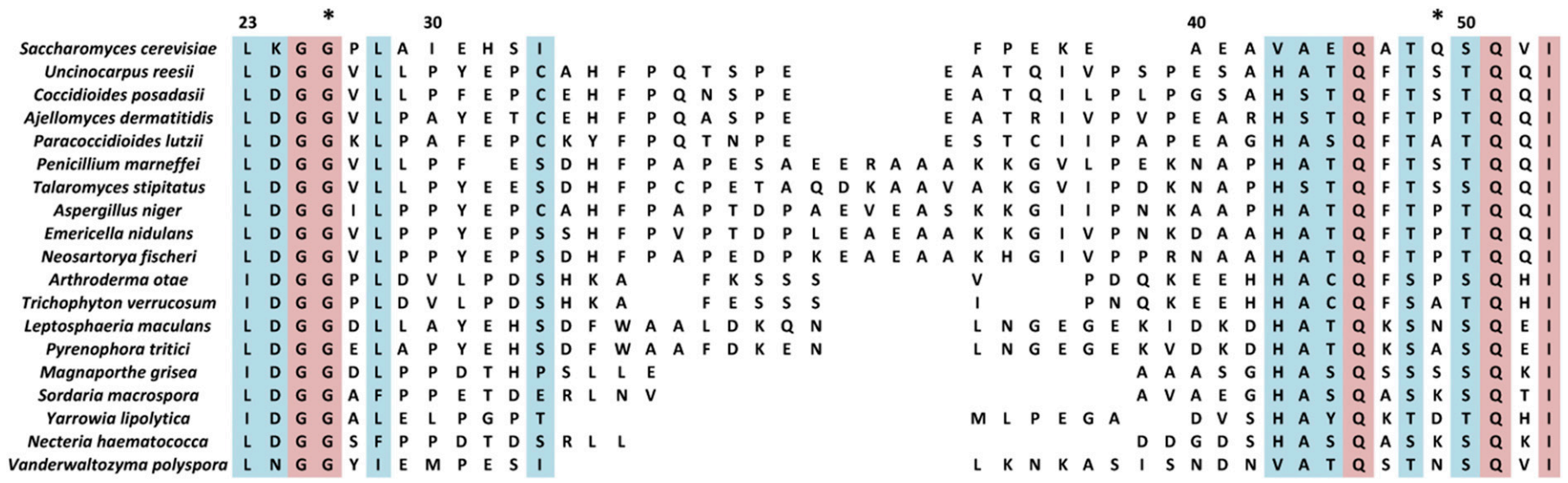

Fig. S7. Sequence alignment of the insert loop common to fungal IGPD homologs. A multisequence alignment for a selection of fungal IGPD homologs that contain the insert between β2 and β3. Numbering is given above for *Sc*_IGPD, and the stars donate the start and end of the insert. Those residues fully conserved are boxed in red; strongly conserved and similar residues are boxed in blue.

Table S1. *Sc*_IGPD 24-mer refinement table from PHENIX

Data collection	Parameter	Value
	Microscope	FEI Titan Krios
	Camera	Falcon III
	Voltage	300 keV
	Pixel size	1.065 Å
	Total dose	~50 $e^-/Å^2$
	Number of frames	39
	Defocus range	0.6–5 μm
	Micrographs	2,827
	Acquisition software	FEI EPU
Image processing		
	Motion correction	MotionCor2
	CTF estimation	Gctf
	Particles selected	365,498
Reconstruction		
	Software	Relion 2.0
	Particles contributed	11,560
	B-factor	−185
	Resolution (FSC 0.143)	3.2 Å
Model building and refinement		
	Model refinement software	Phenix real space
	Map CC (whole unit cell)	0.77
	Map CC (all atoms)	0.80
	rmsd bond length	0.02 Å
	rmsd bond angles	1.22°
	Ramachandran preferred	90.12%
	Ramachandran allowed	9.88%
	Ramachandran outlier	0%
	Rotamer outliers	0%
	C-beta deviations	0
	All-atom clashscore	7.19

Table S2. *At*_IGPD 24-mer refinement table from PHENIX

Data collection	Parameter	Value
	Microscope	FEI Titan Krios
	Camera	Falcon II
	Voltage	300 keV
	Pixel size	1.1 Å
	Total dose	~40 e^{-}/Å^2
	Number of frames	32
	Defocus range	1–3.5 μm
	Micrographs	682
	Acquisition software	SerialEM
Image processing		
	Motion correction	MotionCorr
	CTF estimation	CTFFIND4
	Particles selected	110,977
Reconstruction		
	Software	Relion 1.4
	Particles contributed	55,481
	B-factor	−128
	Resolution (FSC 0.143)	3.1 Å
Model building and refinement		
	Model refinement software	Phenix real space
	Map CC (whole unit cell)	0.63
	Map CC (all atoms)	0.76
	rmsd bond length	0.02 Å
	rmsd bond angles	1.0°
	Ramachandran preferred	91.85%
	Ramachandran allowed	8.15%
	Ramachandran outlier	0%
	Rotamer outliers	0%
	C-beta deviations	0
	All-atom clashscore	4.15